ChemComm

COMMUNICATION

View Article Online
View Journal | View Issue

Cite this: *Chem. Commun.*, 2019, **55**, 13128

Received 27th August 2019,
Accepted 1st October 2019

DOI: 10.1039/c9cc06673j

rsc.li/chemcomm

Light-activated drug release from prodrug nanoassemblies by structure destruction†

Yang Li,‡[a] Shujuan Wang,‡[a] Yulan Huang,[a] Yuwen Chen,[a] Wenbi Wu,[a] Yu Liu,[a] Jing Zhang,[b] Yue Feng,[c] Xian Jiang[d] and Maling Gou *[a]

We report here a novel light-triggered nanosystem based on co-assembling nanoaggregates (NAs) of lipophilic photosensitizers and lipophilic prodrugs containing multiple thioethers. Upon laser irradiation, the oxidization of the multiple thioethers by photosensitizer-generated singlet oxygen could rapidly destroy the NA structure, resulting in faster drug release than those containing a single thioether.

Light-triggered drug release from nanosized drug delivery systems (nanoDDSs) is a promising approach to deliver the encapsulated molecules with a high degree of spatial and temporal control.[1–3] Mediator signals (*e.g.* heat and reactive oxygen species) induced by visible light (400–700 nm) or near-infrared light (700–1000 nm) are widely being utilized to activate drug release.[4–8] However, most light-sensitive systems are constructed based on carrier-assisted nanoDDSs, which suffer severely from their low drug loading capacity (typically 2–10%, w/w).[9] To address this, carrier-free nanoaggregates (NAs) have attracted increasing attention due to their ultrahigh loading capacity.[10,11] Recently, lipophilic prodrugs of hydrophobic drugs (LHPs), despite their highly hydrophobic nature, have been shown to be able to self-assemble into NAs in water.[12,13] As these NAs are constructed with pure prodrugs, their loading capacities are impressively high (~35–70%, calculated in terms of the molecular weights of the parent drug and the prodrug).[13–16] Light-triggered nanoDDSs have been constructed by encapsulating a photosensitizer into NAs of an LHP linked by a single thioether.[17] The mechanism of light-triggered drug release is mainly associated with the singlet oxygen ($^1O_2$)-mediated oxidization of thioether to electron-withdrawing sulfone or sulfoxide, which accelerates the hydrolysis of adjacent ester bonds.[6] However, we found that the light-triggered drug release based on this mechanism was not very sensitive, because the oxidization of a single thioether could not significantly decrease the hydrophobicity of LHPs. Based on this result, we speculated that the light responsiveness would be significantly improved if the hydrophobicity of LHPs could be decreased sharply upon light irradiation. As thioethers are hydrophobic but can be readily oxidized to hydrophilic sulfones or sulfoxides,[18,19] we proposed that insertion of multiple thioethers in LHPs could remarkably decrease the hydrophobicity of the oxidized LHPs, which further resulted in a more sensitive light-triggered drug release as a result of the destruction of the NA structure (Fig. 1A).

To test our hypothesis, we first synthesized the multiple thioether-modified lipophilic prodrug of 7-ethyl-10-hydroxy-camptothecin (SN38) by conjugating two thioether-modified fatty acids at the C_{10} position of SN38 *via* a thioether-containing linker ($2S_2C_{16}$-S/SN38(10), containing 5 thioethers). A lipophobic conjugate of SN38 and stearic acid ($2C_{18}$-S/SN38(10), containing 1 thioether) was utilized as a control. The clinically-approved protoporphyrin IX (PpIX), as a model photosensitizer, was conjugated to stearic acid to obtain C_{18}-S/PpIX. The chemical structures of the lipophilic prodrugs were confirmed by ^{1}H-NMR (Fig. S1–S4, ESI†). When dispersed in water, these lipophilic prodrugs could self-assemble into NAs with average hydrodynamic diameters of 105.2–153.0 nm and negative zeta potentials (Fig. S5, ESI†). Based on their self-assembling abilities, a novel light-triggered nanosystem (5S/SN38(10)-PpIX-NAs) was constructed *via* the co-assembly of $2S_2C_{16}$-S/SN38(10) and C_{18}-S/PpIX at an SN38/PpIX ratio of 8/1 (moles/moles). Co-assembling NAs of $2C_{18}$-S/SN38(10) and C_{18}-S/PpIX (S/SN38(10)-PpIX-NAs) were used for comparative studies to illuminate the role of multiple thioethers in enhancing the responsiveness of light-triggered drug release. As shown in

[a] *State Key Laboratory of Biotherapy and Cancer Center, West China Hospital, Sichuan University, Chengdu, 610041, China. E-mail: goumaling@scu.edu.cn*
[b] *Department of Neurosurgery, West China Hospital, Sichuan University, Chengdu 610041, China*
[c] *The School of Clinical Medicine, Southwest Medical University, Luzhou, Sichuan Province 646000, China*
[d] *Department of Dermatology, West China Hospital, Sichuan University, Chengdu 610041, China*

† Electronic supplementary information (ESI) available: Experimental details, ^{1}H-NMR, SN38 release from SN38(20)-PpIX-NAs, effects of SN38/PpIX ratios on size distributions and oxidization of thioether, effects of irradiation time and power on drug release, and quantum yield of singlet oxygen. See DOI: 10.1039/c9cc06673j

‡ These authors contributed equally to this work.

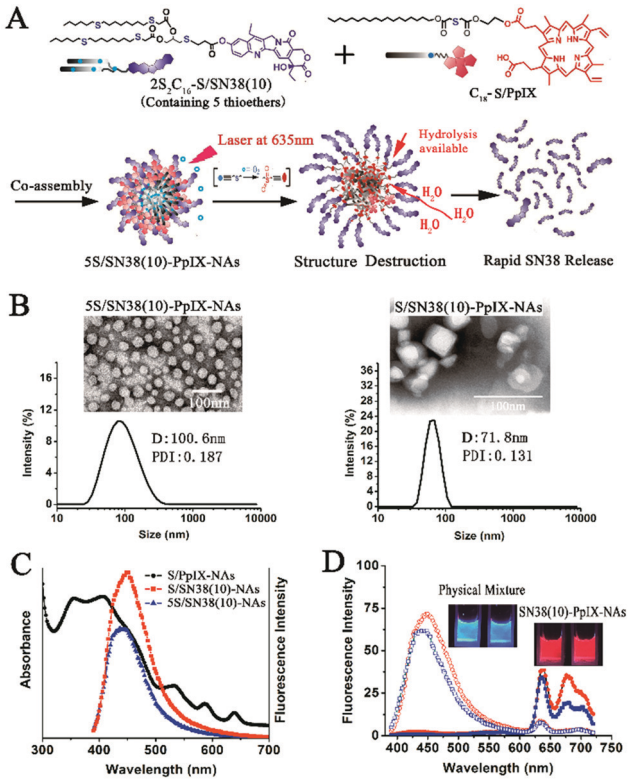

Fig. 1 Schematic illustration of the light-triggered $^1O_2$-activated drug release from the co-assembling NAs of lipophilic PpIX and lipophilic SN38 prodrugs containing multiple thioethers (A). TEM image and size distribution of 5S/SN38(10)-PpIX-NAs and S/SN38(10)-PpIX-NAs (B). Emission spectra of SN38(10)-NAs excited at 362 nm overlapped well with the absorption spectrum of PpIX-NAs, indicating a good FRET pair (C). The emission spectra and pictures under a UV lamp with excitation at 365 nm of SN38(10)-PpIX-NAs and physical mixtures of S/PpIX-NAs and SN38(10)-NAs (D), 10 μg ml^{-1}, SN38 equivalent.

Fig. 1B, transmission electron microscopy (TEM) revealed that the 5S/SN38(10)-PpIX-NAs showed sphere-like shapes, whereas the S/SN38(10)-PpIX-NAs displayed irregular morphologies. Dynamic light scattering (DLS) analysis showed that the 5S/SN38(10)-PpIX-NAs and S/SN38(10)-PpIX-NAs had an average hydrodynamic diameter of 100.6 nm and 71.8 nm, respectively. Based on the molecular weights of SN38 and the prodrugs, the loading capacities of 5S/SN38(10)-PpIX-NAs and S/SN38(10)-PpIX-NAs were calculated to be as high as 32.4% and 34.4%, respectively.

As the emission spectra of $2C_{18}$-S/SN38(10) NAs (S/SN38(10)-NAs) and $2S_2C_{16}$-S/SN38(10) NAs (5S/SN38(10)-NAs) overlapped with the absorption spectrum of C_{18}-S/PpIX NAs (S/PpIX-NAs) (Fig. 1C), the co-assembly of lipophilic prodrugs of SN38 and PpIX could be demonstrated by the fluorescence resonance energy transfer (FRET)-caused quenching of the SN38 fluorescence. As shown in Fig. 1D, both 5S/SN38(10)-PpIX-NAs and S/SN38(10)-PpIX-NAs displayed a red fluorescence under a UV lamp with excitation at 365 nm. Fluorometric analysis showed a complete quenching of the SN38 fluorescence (400–600 nm) and a strong emission spectrum in the wavelength range of 600–740 nm (corresponding to the emission spectrum of PpIX excited at 426 nm, Fig. S6, ESI†), indicating an obvious FRET. By contrast, physical mixtures of S/PpIX-NAs and SN38(10)-NAs displayed a high SN38 fluorescence (Fig. 1D). Such different fluorescent properties indicated the successful co-assembly of lipophilic prodrugs. Unlike the strategy that the photosensitizer was entrapped physically into LHP-NAs, the co-assembly of lipophilic prodrugs could achieve the co-loading of SN38 and PpIX at various SN38/PpIX ratios (Fig. S7, ESI†).

As the FRET signal is very sensitive to the separation distance between the FRET donor and acceptor, the recovery of the SN38 fluorescence can reflect the destruction of the NA structure. The 5S/SN38(10)-PpIX-NAs and S/SN38(10)-PpIX-NAs were exposed to 635 nm irradiation (0.2 W cm^{-2}) for different times; the kinetic changes in SN38 fluorescence were recorded to characterize the destruction of the NA structure. As shown in Fig. 2A, the fluorescence of 5S/SN38(10)-PpIX-NAs changed gradually from red to blue upon irradiation. In contrast, there was fluorescence observed for S/SN38(10)-PpIX-NAs under the same conditions (Fig. 2B). This result was supported by the kinetic changes in the emission spectra: sharply increased SN38 fluorescence for 5S/SN38(10)-PpIX-NAs *versus* the slow increase of SN38 fluorescence for S/SN38(10)-PpIX-NAs (Fig. 2A and B). These results indicated that 5S/SN38(10)-PpIX-NAs were destroyed much more easily than S/SN38(10)-PpIX-NAs upon irradiation. This result was supported by the remarkable change in the size distribution (new signal of larger particles, Fig. S8A, ESI†) of 5S/SN38(10)-PpIX-NAs after irradiation, which has been reported to indicate the destruction of the NA structure.[10] However, TEM did not reveal a different morphology for 5S/SN38(10)-PpIX-NAs after irradiation, in comparison with S/SN38(10)-PpIX-NAs (emergence of many small nanorods, Fig. S8A, ESI†). This result implied that the laser irradiation resulted in the

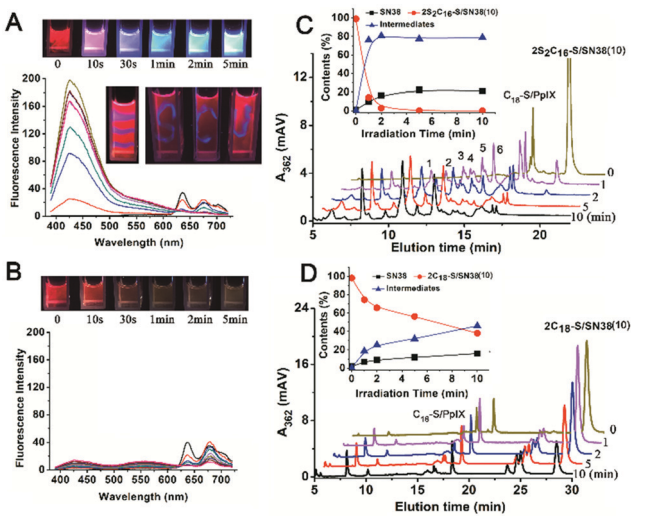

Fig. 2 Kinetic changes in the fluorescence and emission spectra of 5S/SN38(10)-PpIX-NAs (A) and S/SN38(10)-PpIX-NAs (B) with laser irradiation at 0.2 W cm^{-2}. The SN38 fluorescence could be rapidly recovered with 3 s laser irradiation at 0.8 W cm^{-1} for 5S/SN38(10)-PpIX-NAs, which could spell "SCU" in the colloidal solution. Analysis of the degradation of 5S/SN38(10)-PpIX-NAs (C) and S/SN38(10)-PpIX-NAs (D) upon irradiation at 0.2 W cm^{-2}. Insets: Kinetic changes in the peak areas of SN38, the SN38 prodrug and intermediates (expressed as percentages of the total area, 10 μg ml^{-1}, SN38 equivalent).

destruction of the interior structure of 5S/SN38(10)-PpIX-NAs rather than the change in the NA's morphology. To support this, we also found a hypsochromic band shift in the UV-vis spectra of NAs after irradiation (Fig. S8B, ESI†), indicating a less aggregated stage of NAs.[20] We subsequently evaluated the effect of pH, the NA concentration and the power density of irradiation on the recovery of the SN38 fluorescence of 5S/SN38(10)-PpIX-NAs. It is shown that the recovery of the SN38 fluorescence was not remarkably influenced by the pH of the medium, but could be readily suppressed by increasing the concentration of NAs (Fig. S9, ESI†). The SN38 fluorescence was found to increase gradually with laser power (Fig. S10, ESI†), which was explicable because the $^1O_2$ was generated by the photosensitizer in a laser power dependent manner.[6] The SN38 fluorescence could be efficiently activated only with 3 s irradiation at 0.8 W cm^{-2}, which was sensitive enough to spell letters in a colloidal solution of 5S/SN38(10)-PpIX-NAs (Fig. 2A).

High-performance liquid chromatography (HPLC) was then used to monitor the oxidative degradation of $2S_2C_{16}$-S/SN38(10) and $2C_{18}$-S/SN38(10) upon irradiation. As shown in Fig. 2C, after 1 min of irradiation, $2S_2C_{16}$-S/SN38(10) in 5S/SN38(10)-PpIX-NAs was rapidly degraded into SN38 (9.8%) and a series of intermediate products (around 76.0%, marked as **1–6**, showing SN38-like absorption spectra, Fig. S11, ESI†). The oxidized products (**4–6**) could be further oxidized to **1–3** upon longer irradiation. As the irradiation resulted in the disappearance of the peaks of methylene protons in the α-position to thioethers (2.50 and 3.22 ppm), these intermediates were speculated to be the oxidized products of $2S_2C_{16}$-S/SN38(10) as a result of the oxidation of thioethers (Fig. S12, ESI†).[21] In contrast, exposing S/SN38(10)-PpIX-NAs to laser light resulted in a much slower oxidation of $2C_{18}$-S/SN38(10), with only 9.8% of SN38 and 46.1% of the oxidized intermediates obtained after 10 min of irradiation. These results indicated that $2S_2C_{16}$-S/SN38(10) was much more readily oxidized by $^1O_2$ in comparison with $2C_{18}$-S/SN38(10). It is worth mentioning that C_{18}-S/PpIX could be degraded upon irradiation, which agreed well with the decrease of PpIX fluorescence (Fig. 2A and B). We have tried to enhance the oxidation rate of $2C_{18}$-S/SN38 by increasing the amount of C_{18}-S/PpIX. However, the oxidation rate of $2C_{18}$-S/SN38 increased with the amount of C_{18}-S/PpIX only within a certain range; the maximum oxidation rate was achieved at an SN38/PpIX ratio of 16/1 (Fig. S13, ESI†). On the other hand, the oxidation of $2C_{18}$-S/SN38(10) in S/SN38(10)-PpIX-NAs was much faster than that in the physical mixture of S/SN38(10)-NAs and S/PpIX-NAs (oxidized product, 46.1% *versus* 17.2%) (Fig. S14, ESI†), implying that the co-assembly of lipophilic prodrugs was the prerequisite for the rapid oxidation of thioether. As $2C_{18}$-S/SN38 could be oxidized by the indocyanine green-generated $^1O_2$ upon irradiation at 808 nm (Fig. S15, ESI†), such a light-sensitive nanosystem could also be constructed based on photosensitizers in the near-infrared window.

To verify whether the fast oxidation of $2S_2C_{16}$-S/SN38(10) could result in a more sensitive light-triggered SN38 release, the laser-treated NAs were incubated at 37 °C in 10 mM phosphate buffer (PB, pH 7.4) and the sample was withdrawn for HPLC analysis. As shown in Fig. 3A, $2S_2C_{16}$-S/SN38(10) after 5 min of irradiation

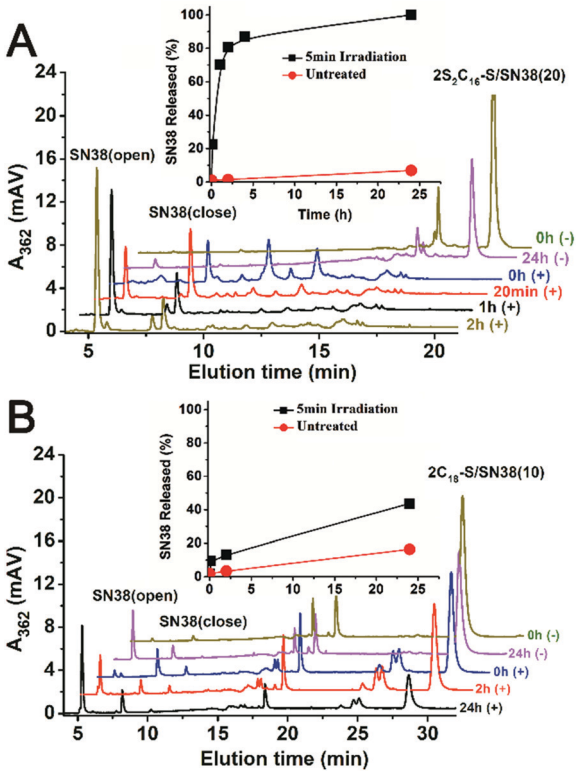

Fig. 3 Cumulative SN38 release from 5S/SN38(10)-PpIX-NAs (A) and S/SN38(10)-PpIX-NAs (B) without irradiation (–) or after 5 min of irradiation (+) at 0.2 W cm^{-2}, 10 μg ml^{-1}, SN38 equivalent.

was rapidly converted to SN38 (80.7% within 2 h), which was remarkably higher than that without irradiation (6.8% within 24 h). For S/SN38(10)-PpIX-NAs, $2C_{18}$-S/SN38(10) remained relatively stable, resulting in 43.7% SN38 release in 24 h. This release was only around 2.7-fold faster than that without irradiation, indicating poor light sensitivity. These results implied that 5S/SN38(10)-PpIX-NAs showed a much more sensitive light-triggered SN38 release than S/SN38(10)-PpIX-NAs. To evaluate the effect of the conjugate position of the lipid-SN38 prodrug on light-triggered SN38 release, lipophilic SN38 prodrugs were also synthesized by conjugating fatty acids at the C_{20} position of SN38 (*i.e.* $2S_2C_{16}$-S/SN38(20) and $2C_{18}$-S/SN38(20), ^{1}H-NMR shown in Fig. S16, ESI†). These prodrugs were then co-assembled with C_{18}-S/PpIX to obtain 5S/SN38(20)-PpIX-NAs and S/SN38(20)-PpIX-NAs, which only displayed 16.8% and 1.7% SN38 release within 24 h after 5 min of irradiation, respectively (Fig. S17, ESI†). These values were significantly lower than that of SN38(10)-PpIX-NAs, which might be ascribed to the high hydrolytic stability and great steric hindrance around the ester bond at C_{20}.[22] Despite this, 5S/SN38(20)-PpIX-NAs still achieved around 10-fold faster SN38 release than S/SN38(20)-PpIX-NAs, indicating that the presence of multiple thioethers significantly enhanced the sensitivity of SN38 release triggered by the light irradiation.

Interestingly, the degradation of the oxidized products of $2S_2C_{16}$-S/SN38(10) was correlated highly with their retention time in the chromatographic curve (Fig. S18, ESI†), indicating that the oxidized products having a higher hydrophilicity were more readily

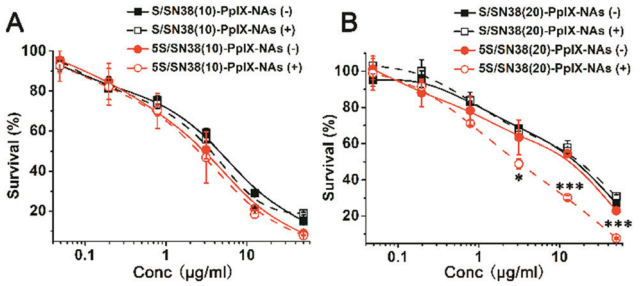

Fig. 4 Cytotoxicities of SN38(10)-PpIX-NAs (A) and SN38(20)-PpIX-NAs (B) without irradiation (–) or after 1 min of irradiation (+) at 0.4 W cm^{-2}, [means ± SD, $n = 4$], $*p < 0.05$, $***p < 0.001$.

converted to SN38. This result suggested that the rapid SN38 release from the light-irradiated 5S/SN38(10)-PpIX-NAs might be ascribed to the increased hydrophilicity of the oxidized products, which made them more available for hydrolysis. It is worth mentioning that the SN38 release from 5S/SN38(10)-PpIX-NAs was dependent on the irradiation time (Fig. S19, ESI†). The SN38 release increased with irradiation time, approaching equilibrium after 5 min at a power of 0.2 W cm^{-2}. Similarly, increasing the irradiation power could also accelerate the degradation of $2S_2C_{16}$-S/SN38, further resulting in a faster SN38 release (Fig. S20, ESI†).

We then investigated the *in vitro* cytotoxicity of these NAs on CT26 colonic cancer cells using MTT assay. As shown in Fig. 4A, both 5S/SN38(10)-PpIX-NAs and S/SN38(10)-PpIX-NAs showed similar cytotoxicity (IC_{50}, 2.1–3.7 μg ml^{-1}), irrespective of whether irradiation was applied or not. This was probably ascribed to the rapid hydrolysis of phenolic ester in culture medium, which significantly decreased the selectivity of light-triggered SN38 release (Fig. S21A, ESI†). For 5S/SN38(20)-PpIX-NAs containing a stable ester linker at C_{20}, light irradiation resulted in around 5-fold higher SN38 release in the culture medium (Fig. S21B, ESI†), resulting in a higher cytotoxicity (IC_{50}, 9.3 *versus* 3.2 μg ml^{-1}, Fig. 4B). In contrast, S/SN38(20)-PpIX-NAs displayed poor cytotoxicity, due to the poor SN38 release both in the presence and in the absence of irradiation. Interestingly, S/PpIX-NAs showed a much poorer light-induced cytotoxicity (<100 fold) than free PpIX (Fig. S22, ESI†). As S/PpIX-NAs displayed a comparable quantum yield of $^1O_2$ to free PpIX (Fig. S23, ESI†), the poor cytotoxicity of S/PpIX-NAs was probably due to their heterogeneous distributions in cells, which limited oxidative reactions between the short-lived $^1O_2$ (could only diffuse 10–20 nm) and adjacent biological macromolecules.[23] Therefore, the cytotoxicity of SN38-PpIX-NAs mainly arose from the released SN38 rather than the phototoxicity of PpIX.

In conclusion, a novel light-responsive nanosystem based on co-assembling NAs of thioether-modified lipophilic prodrugs of SN38 and PpIX was developed. Upon 635 nm red light irradiation, PpIX can generate $^1O_2$ to oxidize hydrophobic thioether *in situ* to hydrophilic sulfone, and thus to accelerate SN38 release. We demonstrated that the presence of multiple thioethers significantly enhanced the sensitivity of SN38 release triggered by the light irradiation, due to the destruction of the interior structure of NAs. Importantly, our preliminary data suggested that such NAs could be constructed based on photosensitisers that can be activated by near-infrared light, which holds potential for future clinical applications. Moreover, these NAs were constructed simply by the co-assembly of the two lipophilic prodrugs, which displayed many advantages, such as the controllable co-assembling drug ratio, high loading capacity, one-step preparation and sensitive light responsiveness to drug release. These benefits endow them with great potential to serve as promising nanocarriers for the spatially and temporally selective delivery of antitumor drugs.

This research was supported by the key research and development projects of people's liberation army (BWS17J036), the 1·3·5 project for disciplines of excellence, West China Hospital, Sichuan University (ZYYC08007, ZYJC18017) and the Science and Technology Project of Chengdu (2018-CY02-00041-GX).

Conflicts of interest

There are no conflicts to declare.

Notes and references

1 Y. Zhou, H. Ye, Y. B. Chen, R. Y. Zhu and L. C. Yin, *Biomacromolecules*, 2018, **19**, 1840–1857.
2 Y. F. Li, Y. M. Zhang and W. P. Wang, *Nano Res.*, 2018, **11**, 5424–5438.
3 E. R. Ruskowitz and C. A. DeForest, *Nat. Rev. Mater.*, 2018, **3**, 17087.
4 W. Tao, X. Ji, X. Zhu, L. Li, J. Wang, Y. Zhang, P. E. Saw, W. Li, N. Kong, M. A. Islam, T. Gan, X. Zeng, H. Zhang, M. Mahmoudi, G. J. Tearney and O. C. Farokhzad, *Adv. Mater.*, 2018, **30**, 1802061.
5 X. Ji, N. Kong, J. Wang, W. Li, Y. Xiao, S. T. Gan, Y. Zhang, Y. Li, X. Song, Q. Xiong, S. Shi, Z. Li, W. Tao, H. Zhang, L. Mei and J. Shi, *Adv. Mater.*, 2018, **30**, 1803031.
6 C. G. Dariva, J. F. J. Coelho and A. C. Serra, *J. Controlled Release*, 2019, **294**, 337–354.
7 A. Sanchis, J. P. Salvador and M. P. Marco, *Colloids Surf., B*, 2019, **173**, 825–832.
8 J. M. Silva, E. Silva and R. L. Reis, *J. Controlled Release*, 2019, **298**, 154–176.
9 S. Y. Qin, A. Q. Zhang, S. X. Cheng, L. Rong and X. Z. Zhang, *Biomaterials*, 2017, **112**, 234–247.
10 L. Minghui, S. Xuetan, Z. Ning, W. Wei, Y. Yang, J. Huizhen and L. Wenguang, *Adv. Sci.*, 2018, **5**, 1800155.
11 N. Zhang, M. Li, X. Sun, H. Jia and W. Liu, *Biomaterials*, 2018, **159**, 25–36.
12 Y. Li, T. Kang, Y. Wu, Y. Chen, J. Zhu and M. Gou, *Chem. Commun.*, 2018, **54**, 1996–1999.
13 Y. J. Wang, D. Liu, Q. C. Zheng, Q. Zhao, H. J. Zhang, Y. Ma, J. K. Fallon, Q. Fu, M. T. Haynes, G. M. Lin, R. Zhang, D. Wang, X. G. Yang, L. X. Zhao, Z. G. He and F. Liu, *Nano Lett.*, 2014, **14**, 5577–5583.
14 C. Luo, J. Sun, D. Liu, B. J. Sun, L. Miao, S. Musetti, J. Li, X. P. Han, Y. Q. Du, L. Li, L. Huang and Z. G. He, *Nano Lett.*, 2016, **16**, 5401–5408.
15 C. Luo, J. Sun, B. Sun, D. Liu, L. Miao, T. J. Goodwin, L. Huang and Z. He, *Small*, 2016, **12**, 6353–6362.
16 H. Wang, H. Xie, J. Wang, J. Wu, X. Ma, L. Li, X. Wei, Q. Ling, P. Song, L. Zhou, X. Xu and S. Zheng, *Adv. Funct. Mater.*, 2015, **25**, 4956–4965.
17 B. Yang, K. Wang, D. Zhang, B. Sun, B. Ji, L. Wei, Z. Li, M. Wang, X. Zhang, H. Zhang, Q. Kan, C. Luo, Y. Wang, Z. He and J. Sun, *Biomater. Sci.*, 2018, **6**, 2965–2975.
18 F. H. Sobotta, F. Hausig, D. O. Harz, S. Hoeppener, U. S. Schubert and J. C. Brendel, *Polym. Chem.*, 2018, **9**, 1593–1602.
19 J. Yoo, N. S. Rejinold, D. Lee, S. Jon and Y.-C. Kim, *J. Controlled Release*, 2017, **264**, 89–101.
20 I. Nabiev, F. Fleury, I. Kudelina, Y. Pommier, F. Charton, J. F. Riou, A. J. P. Alix and M. Manfait, *Biochem. Pharmacol.*, 1998, **55**, 1163–1174.
21 J. Wang, X. Sun, W. Mao, W. Sun, J. Tang, M. Sui, Y. Shen and Z. Gu, *Adv. Mater.*, 2013, **25**, 3670–3676.
22 A. G. Cheetham, Y.-C. Ou, P. Zhang and H. Cui, *Chem. Commun.*, 2014, **50**, 6039–6042.
23 D. K. Chatterjee, L. S. Fong and Y. Zhang, *Adv. Drug Delivery Rev.*, 2008, **60**, 1627–1637.